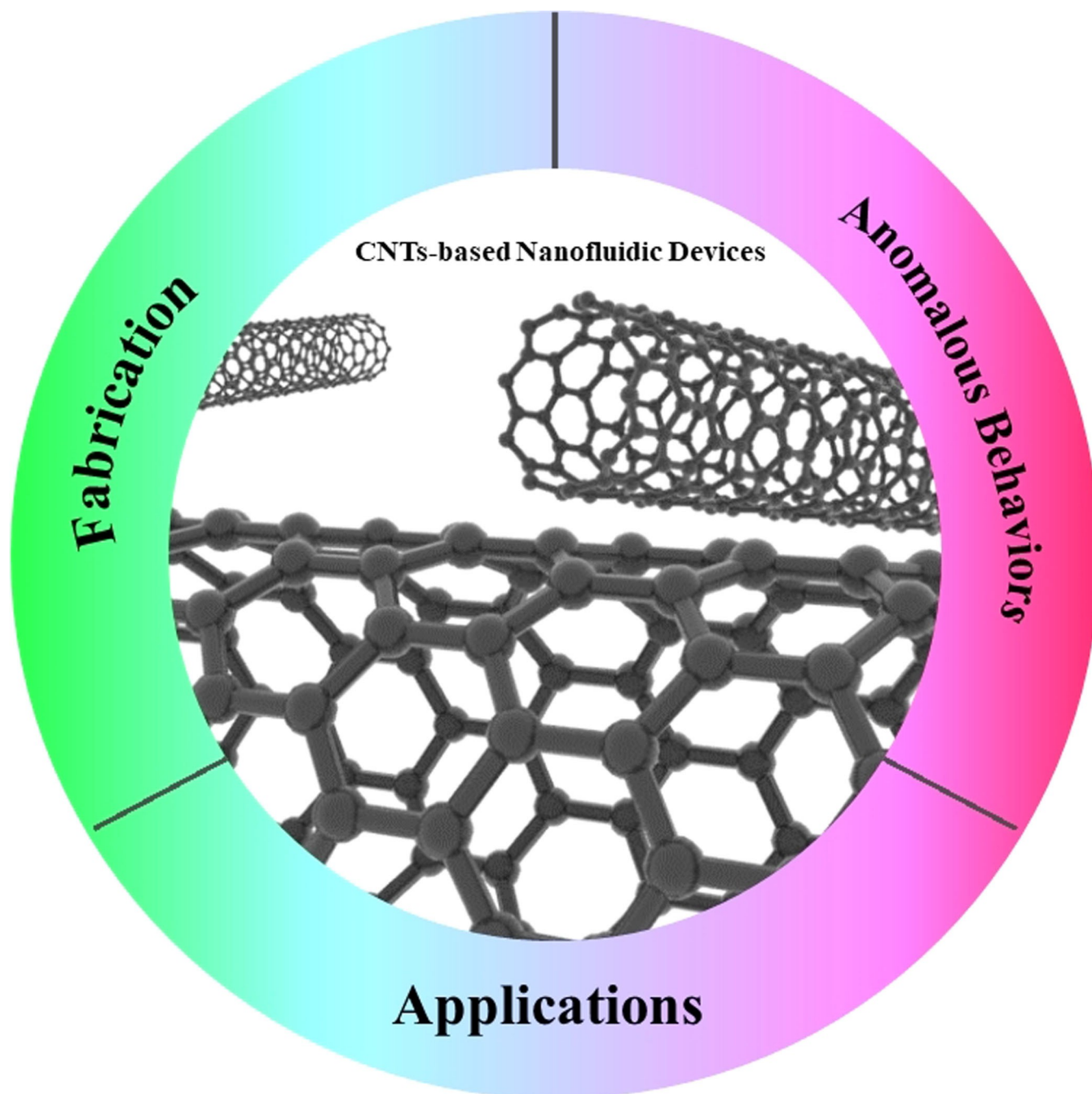




Carbon Nanotubes-Based Nanofluidic Devices: Fabrication, Property and Application

Haoyang Zhou,^[a, b] Weiqi Li,^{*[a, b]} and Ping Yu^{*[a, b]}



With the rapid development of nanofluidics, more and more unexpected behaviors and bizarre properties have been discovered, which brings more possibility to solve the water and energy problem. Carbon nanotubes (CNTs) with nanoscale diameter and ultrasmooth hydrophobic surface provide strong confinement and unusual water-carbon couple which lead to

many exotic properties, such as flow enhancement, strong ion exclusion, ultrafast proton transport and phase transition. This article reviews the recent progresses of CNT-based nanofluidic devices in fabrication, property, and applications. Moreover, challenges and opportunities of the CNT-based nanofluidic devices are discussed.

1. Introduction

In recent years, nanofluidics have been more widely studied for exploring the special transport of fluids and ions in the nanometer channels. Over the past twenty years, various abnormal behaviors of fluids and ions in the nanoscale channels, which depart from continuum expectations in many aspects, have been discovered, such as the greatly increased flow,^[1] the abnormal dielectric permittivity of water,^[2] the ionic Coulomb blockade behavior^[3] and so on. This benefits not only from the development of nanofabrication technologies, which make it possible to fabricate artificial channels at nanometer or even sub-nanometer scale, but also from the advances in techniques and instruments for ion transport investigation.^[4] These studies open up new avenues for diverse potential applications of nanofluidics, such as membrane science for seawater desalination,^[5] osmotic energy conversion,^[6] unique chemical sensing devices^[7] and artificial cell construction.^[8]

The emergence of new nanomaterials boosts the rapid development of nanofluidics and provides potential platforms for the experimental characterization and theoretical simulation of nanofluids.^[4] So far, various nanomaterials, including one-dimensional (1D) and two-dimensional (2D) materials, have been used to fabricate nanofluidic devices. The 1D materials mainly refer to carbon nanotubes (CNTs) and boron nitride nanotubes (BNNTs). The device fabrication methods with 1D materials could be divided into deposition and insertion methods, which will be discussed in this review. 2D materials have been developed into a big family ranging from traditional 2D materials including graphene, boron nitride (BN), and molybdenum disulfide (MoS₂) to new 2D materials such as zeolites, metal-organic framework (MOF) nanosheets, graphene

oxide, clay and MXenes made of transition metals.^[9] In the meantime, various methods have been developed for the construction of nanofluidic devices using 2D materials. Nanopores and nanochannels on 2D materials are able to provide nanometric confinement for fluids. For nanopores, they can be constructed by porous 2D materials with intrinsic pores or artificial holes prepared by a focused ion beam (FIB) drilling.^[10] Nanochannels can be prepared by assembling nanosheets into laminates due to the relatively weak interlayer van der Waals force.^[11] Esfandiari *et al.* has successfully applied this Lego-like method in the fabrication of nanofluidic devices with three kinds of materials including graphite, BN and MoS₂.^[12] An array of graphene spacers was used to separate the top flat crystal from the bottom one, thus providing smooth walls and channels with atomic-scale precision to study water transport.


Distinct from other nanomaterials, there is a bizarre coupling only exists at the interface of water and carbon materials which results in various unique phenomena such as ultrafast water flow and phase transitions. These phenomena not only challenge the traditional theories but also bring potential opportunities for the application of carbon materials. However, the preparation of 2D carbon materials still faces big challenges such as the limitation in monolayer exfoliation and controllable perforation. From this point of view, 1D CNTs with smooth hydrophobic inner walls and nanometer-scale diameter, are ideal channel platform to investigate the nanofluidic behaviors. So far, theoretical and experimental studies have reported many interesting phenomena using diverse CNT-based nanofluidic devices. Some reports have reviewed the mass transport under nanoscale confinement with various nanomaterials in experimental setups and theoretical simulations.^[13] Herein, we focus on the significant progresses of CNT-based nanofluidic devices, and would like to provide a more comprehensive review in terms of the device fabrication, more abnormal fluid behaviors and their applications.


2. Fabrication of CNTs-Based Nanofluidic Devices

Despite the benefits of CNTs in the study of nanofluids due to its unique structure and properties, the fabrication of CNT-based nanofluidic devices, especially devices with one single CNT, still remains a challenge. With the improvement of nanofabrication, more and more studies have reported the construction of CNT-based experimental devices and platforms. Here, two typical construction methods of CNT-based nano-

[a] H. Zhou, W. Li, Prof. Dr. P. Yu
Beijing National Laboratory for Molecular Sciences
Key Laboratory of Analytical Chemistry for Living Biosystems
Institute of Chemistry
Chinese Academy of Sciences
Beijing 100190 (P. R. China)

[b] H. Zhou, W. Li, Prof. Dr. P. Yu
University of Chinese Academy of Sciences
Beijing 100049 (P. R. China)
E-mail: liweiqi@iccas.ac.cn
yuping@iccas.ac.cn

 Part of a joint Special Collection of ChemistryOpen, Analysis & Sensing and Chemistry-Methods focusing on "Biosensing and Imaging: Methods and Applications". Please visit chemistryopen.org/collections to view all contributions.

 © 2022 The Authors. Published by Wiley-VCH GmbH. This is an open access article under the terms of the Creative Commons Attribution Non-Commercial NoDerivs License, which permits use and distribution in any medium, provided the original work is properly cited, the use is non-commercial and no modifications or adaptations are made.

fluidic devices are summarized including deposition and insertion methods.

2.1. Deposition Method

The deposition method, composed of in situ deposition of CNTs on an inert substrate followed by the creation of nanochannels between the chambers at both ends of CNTs and then dices to form nanochannels between the chambers, was developed by Strano *et al.*^[14] They synthesized ultralong aligned single-walled carbon nanotubes (SWNTs) by chemical vapor deposition on a silicon wafer and then removed unnecessary parts by plasma etching to open both ends of nanotubes (Figure 1a). The ionic current through the nanotubes is monitored by filling the compartments with salt solution. Besides, Liu *et al.*^[15] also applied the deposition method by using ethanol vapor as carbon source to grow CNTs on silicon substrate and oxygen plasma etch to remove the exposed parts of CNTs. The parts under the barrier were retained to connect the two fluid reservoirs for measuring the ion transport and electrophoretic transport of DNA. Specifically, the deposition methods composed of CNT-fabrication and photolithography techniques make it easier to control the number and length of the CNTs involved.

2.2. Insertion Method

CNT-based nanofluidic devices can also be constructed by physically inserting CNTs into polymer films or lipid bilayers. Crooks *et al.*^[16] embedded a single CNT within an epoxy block and subsequently prepared the nanopore membranes containing CNT nanopores by efficiently cutting. A piece of CNT membranes was fixed on the support to separate two cells, and the mass transport was recorded by measuring the current pulse induced by probes blocking. This approach can be used to prepare a series of membranes with well-defined geometric

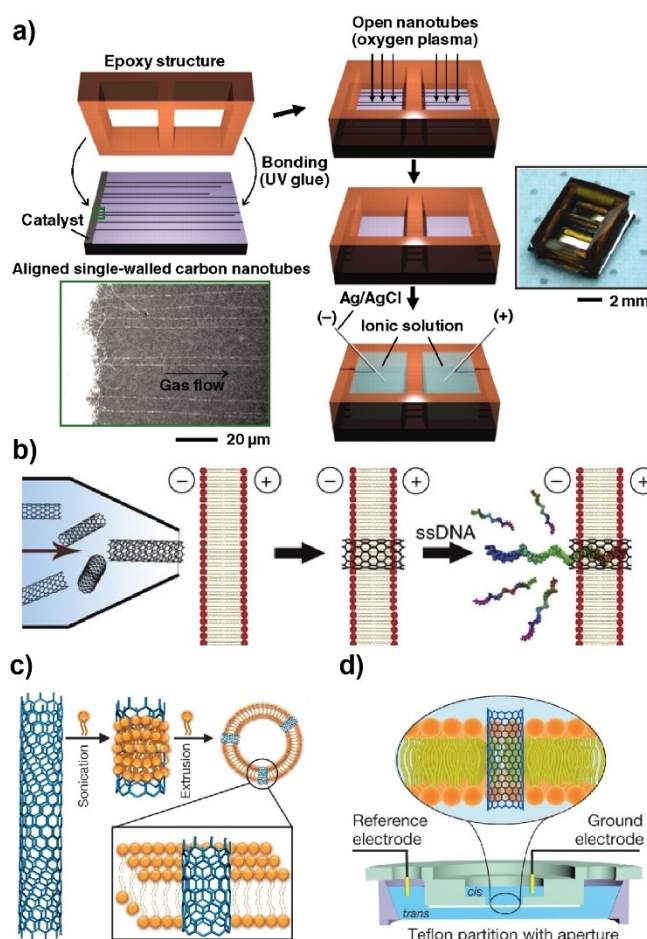


Figure 1. Experimental devices of CNT-based nanochannel. a) Fabrication of deposited CNTs ion channels. Reproduced with permission from Ref. [14], Copyright 2010, AAAS. b) Insertion of a SWNT into lipid bilayer by injection and the process of single-stranded DNA (ssDNA) translocation. Reproduced with permission from Ref. [17], Copyright 2013, Springer Nature. c) Ultrashort CNT preparation and its incorporation into liposomes. Reproduced with permission from Ref. [18], Copyright 2014, Springer Nature. d) Experimental set-up of the single-channel conduction recording. Reproduced with permission from Ref. [18], Copyright 2014, Springer Nature.



Haoyang Zhou received her Bachelor's degree from the East China University of Science and Technology in 2020. She is currently a PhD candidate under the supervision of Prof. Ping Yu in the Institute of Chemistry, Chinese Academy of Sciences. Her research interests mainly focus on the sensing and regulation in brain chemistry.



Weiqi Li received her bachelor's degree from Shandong University in 2016 and master's degree from ICCAS in 2019. Now she is currently a PhD student at ICCAS, working on the ion transport behavior based on graphdiyne.



Ping Yu is currently a professor in the Key Laboratory of Analytical Chemistry for Living Biosystems at Institute of Chemistry, the Chinese Academy of Sciences. She received her PhD in Chemistry from Institute of Chemistry, the Chinese Academy of Sciences in 2007 and then worked in the same institute. She was a recipient of the "National Outstanding Young Scholars" from the National Natural Science Foundation of China. Her research interests focus on ion transport, electrochemistry, chem/(bio) sensors and in vivo analysis.

and chemical nanopore and enhances the measurement reproducibility. Wu *et al.*^[17] firstly injected ultrashort CNTs directly into lipid bilayers (Figure 1b) and measured the ionic current through CNTs to detect the molecules transport. The device exhibited stable baseline and high signal-to-noise ratio, which displayed many interesting phenomena about ion and nucleic acid transport. Based on the similar strategy, Noy *et al.*^[18] prepared ultrashort CNTs coated with phospholipids by sonication, which could automatically insert into the lipid bilayer membranes and living cell membranes (Figure 1c, d). The phospholipid-coated CNTs were further inserted into membrane of liposomes and the ion transport was measured by the response of fluorescence probe.^[19] All these experimental facilities provide promising platforms for studying the special properties of nanofluids and the insertion method is more beneficial for the construction of devices with single CNT.

3. Anomalous Behaviors of CNTs-Based Nanofluidic Devices

3.1. Fluidic flow enhancement

The frictionless surface of the inner CNTs wall contributes to high fluid velocity of water transport inside the CNTs. This high

fluid velocity can be explained by the ultralong slip lengths which is an extrapolation of the extra pore radius required to give zero velocity at a hypothetical pore wall.^[20] Researches on the slip flow enhancement in CNTs have received high attention since the early 2000s and achieved explosive growth over the past two decades. In 2001, Hummer *et al.*^[21] reported that CNTs with rigid nonpolar structures can be spontaneously and continuously filled with 1D water molecules ordered chain by using molecular dynamics (MD) simulations. Three factors including ordered hydrogen bonds, weak attraction between water molecules and the smooth CNT walls lead to the fast water flow with small resistance. Based on this theory, Majumder *et al.*^[22] reported that the slip length of water in 7 nm-diameter CNT membrane ranges from 39,000 to 68,000 nm. And Holt *et al.*^[11] reported that the slip length in sub-2 nm-diameter CNT film is 140–1400 nm. Since these studies mostly utilized CNT membranes instead of individual CNT of which the utilization needs to overcome enormous technical challenges, early mechanistic explanations of fast water transport in CNTs are highly controversial.

The measurement of water flow in a single CNT was successfully achieved by Secchi *et al.*^[23] by sealing a CNT at the tip of a glass nanocapillary. The permeability of the nanotube was calculated using the external flow induced by the fluid jet (Figure 2a). It was reported that the slip length is closely related to the diameter of CNTs. The smaller the diameter is, the larger

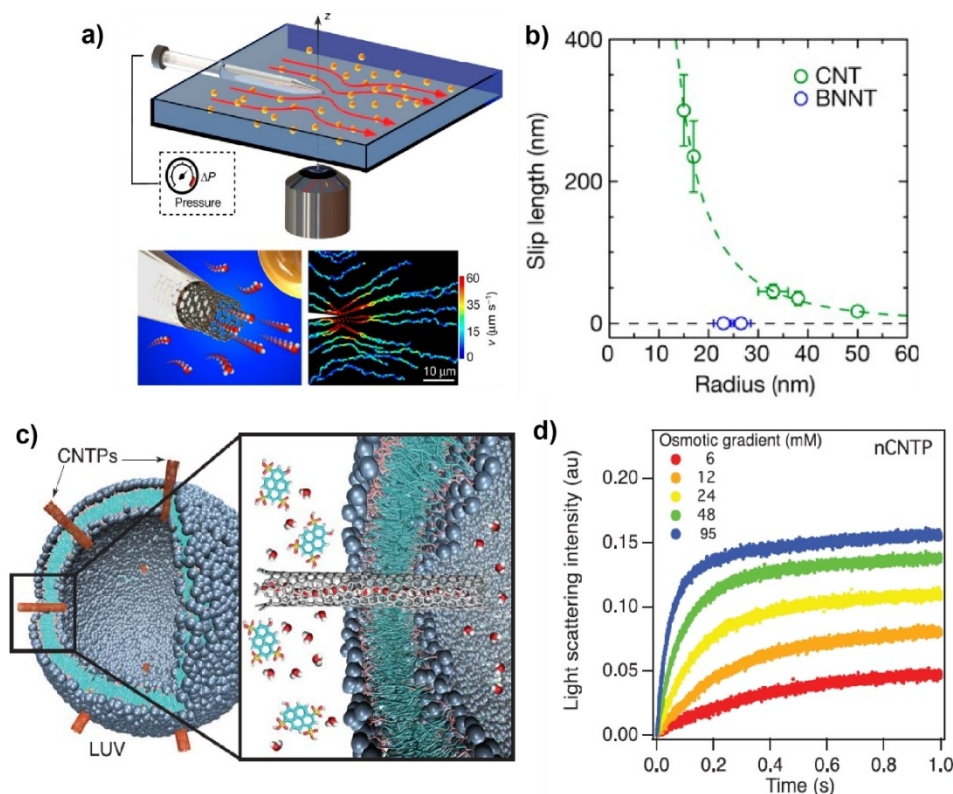


Figure 2. Fluidic flow enhancement. a) Nanojets emerging from individual nanotubes to image the Landau–Squire flow. Reproduced with permission from Ref. [23], Copyright 2016, Springer Nature. b) Radius dependence of the slip length of individual CNTs and BNNTs. Reproduced with permission from Ref. [23], Copyright 2016, Springer Nature. c) Water transport in CNTs embedded in large unilamellar vesicles. Reproduced with permission from Ref. [24], Copyright 2017, AAAS. d) Light-scattering traces recorded after subjecting lipid vesicles containing narrow CNTs with the varying of osmotic gradients. Reproduced with permission from Ref. [24], Copyright 2017, AAAS.

the slip length would enhance. However, BNNTs which is similar with the crystallography of CNTs, showed no slippage (Figure 2b). This difference was attributed to their radically different electronic properties since BNNTs are insulating in contrast to semi metallic CNTs. This result demonstrated that the atomic-scale details of the solid-liquid interface, such as electronic properties, could make dramatic differences in fluid behaviors. Noy *et al.* also measured the water flow inside the CNTs by a completely different approach.^[24] They used ultrashort CNTs that can spontaneously insert into the walls of large unilamellar vesicles to form transmembrane channels. When the vesicles were exposed to a hypertonic buffer solution, they shrank due to the osmotic gradient driving water efflux. According to the Rayleigh-Gans-Debye theory of light scattering, the reduction of the vesicles volume caused the increase of the light scattering intensity (Figure 2c, d). And the water permeabilities of individual CNT could be extracted from the data. The results showed that the permeability of narrow CNTs (0.8 nm in diameter) was 11 times higher than that of wider CNTs (1.5 nm in diameter) and was even 6 times higher than that of

Aquaporin-1 (water selective biological protein nanochannel). Based on MD simulation, a microscopic description is provided to explain the ultrafast water transport in narrow CNTs: the water molecules arrange into a 1D linear chain forced by the strongly confined space and hydrophobic inner wall of narrow CNTs, whereas water in wider CNTs resembles the bulk state.

3.2. Special ion transport

The strong CNT confinement also gives rise to interesting physical phenomena of ion transport. The confined 1D linear chain water molecules in the 0.8 nm-diameter channel also shows an abnormal fast proton transport efficiency.^[19] Unilamellar vesicles containing a pH sensitive fluorescence probe (Pyranine) and embedded with ultrashort CNTs were used to measure the proton permeability (Figure 3a). After rapid acidification of the external solution, the osmotic balance was broken and the proton fluxed through the CNTs, leading to the decrease of the encapsulated dye fluorescence (Figure 3b). The

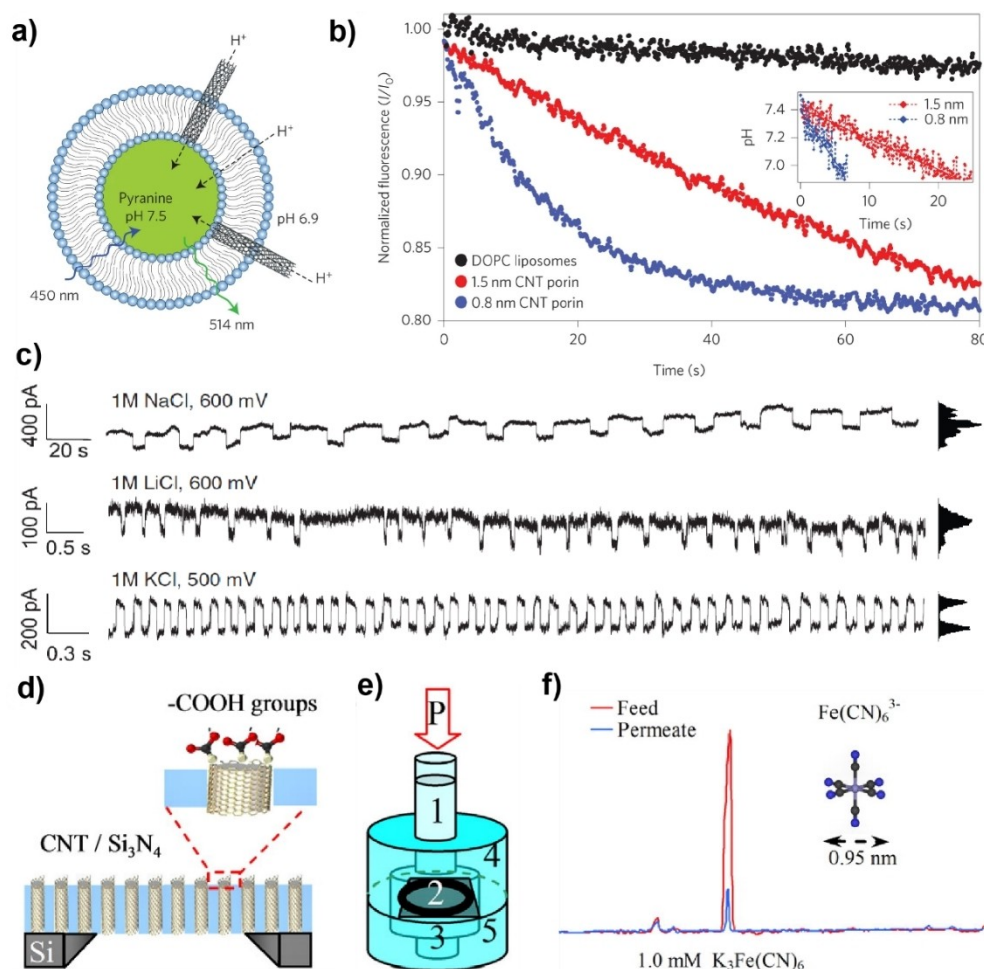


Figure 3. Special ion transport in CNTs. a, b) Proton conduction in CNTs. Reproduced with permission from Ref. [19], Copyright 2016, Springer Nature. a) Schematic of the proton conductance measurement. b) Normalized fluorescence intensity changes as a function of time showing the proton transport rate. Reproduced with permission from Ref. [19], Copyright 2016, Springer Nature. c) Metastable oscillations of the electroosmotic current depending on the position of the pore blocker. Reproduced with permission from Ref. [14], Copyright 2010, AAAS. d-f) Ion exclusion of sub-2 nm wide CNT membrane. Reproduced with permission from Ref. [26], Copyright 2008, National Academy of Sciences.

measured proton diffusion constant for 0.8 nm CNTs, $4.20 \pm 0.91 \text{ \AA}^2 \text{ ps}^{-1}$, is much larger than that of proton transport in bulk water ($0.4 \text{ \AA}^2 \text{ ps}^{-1}$), which could be explained by the Grotthuss 'hop-turn' mechanism.^[25] The results also illustrate the potential application of CNTs as proton conductor in the field of energy transduction.

In addition to the ultrafast proton transport, SWNTs channels exhibit signatures of coherent resonance,^[14] in which the electroosmotic current through the interior of SWNTs shows oscillations under a specific range of electric fields (Figure 3c). These oscillations are thought to be caused by the coupling between the stochastic pore blocking and the proton-diffusion limitation at the pore mouth. The protons at the pore mouth depleted due to the large proton fluxes which in turn increases the relative concentration of ions. The ion concentration difference leads ions migrate into the CNTs and then cause blockage. After the blocking, the proton concentration at the pore mouth increases again which makes the proton current restore back at the same time to form a cycle. This system provides an alternative to the emerging family of devices that use ions for information processing as an ionic resonator or waveform generator.

The narrow CNTs also exhibit significant ion exclusion due to steric hindrance, interaction with pore walls and electrostatic interactions. Researchers have used CNT membranes to investigate ion transport and found a strong ion rejection of the membranes.^[26] They used vertically aligned CNTs to fabricate sub-2 nm CNT membranes and constructed a nanofluidic platform on silicon nitride (Figure 3d). After etching, hydroxyl, carbonyl and carboxylic functional groups were introduced at the rim of CNTs. These negatively charged carboxyl groups make the electrostatic interactions dominate the ionic exclusion of CNT films. A pressure-driven nanofiltration cell was used to quantify the ion rejection (Figure 3e). The cell was divided into two parts by a CNT membrane, feed part (top) and permeate part (bottom). Salt solution filled the feed chamber and was pressurized at $p = 0.69$ bar to permeate through the membrane. The ion concentration in permeate solutions and feed solutions was analyzed by capillary electrophoresis. Compared the chromatogram of the feed (red) and permeate (blue) solution, a 91% exclusion of the ferricyanide anion after filtration of a 1.0 mM potassium ferricyanide solution was calculated (Figure 3f). By observing the sensitivity of ion rejection dependency of the pH and Debye length, they found that the mechanism of significant ion rejection was related to the electrostatic interactions. In 2017, Noy *et al.* measured the ion transport inside single sub-nanometer CNT by using lipid bilayer platform and further demonstrated that the negative charge at the rim of CNT results in good ion exclusion.^[5] Unlike previous studies, they found that strong anion exclusion property of 0.8 nm-diameter CNTs can still persist even at 1 M salinity levels, which also offers the possibility to develop ultra-permeable membranes for water purification.

Except for ion exclusion, simulations and experiments have revealed many patterns of ion selectivity in CNTs. For example, permeation of small ions through CNTs driven by concentration have been researched by using SWNTs membranes.^[27] It

reported that the ion diffusion rate through CNTs was far above the permeation through the bulk that was typically assumed to follow. Besides, strong difference up to two orders of magnitude in permeability of monovalent anions through narrow CNTs was found.^[28] LUVs with CNTs embedded containing lucigenin dyes (halide ion-sensitive dyes) were mixed with solutions. When the halide anions transport into the LUVs causing the quenching of dyes, a decrease of fluorescence would be recorded by the stopped-flow spectrometer and the anion flux can be measured. The trend of permeability of four anions clearly follows the Hofmeister series ($\text{SCN}^- > \text{I}^- > \text{Br}^- > \text{Cl}^-$). The physical origin of these phenomena still cannot be interpreted systematically. As mentioned above, negatively charged carboxyl groups at the rim are supposed to be a part of the reason but not inadequate. Ion transport inside a single CNT has been studied to explore the origin. Hydroxide adsorption at the surface of the CNTs,^[29] strong coupling between water and ions in CNTs^[30] and ion dehydration energy^[28] also need to be taken into account.

3.3. Phase transition

The nanoscale hollow interiors of CNTs which could be used as a template for material encapsulation intrigues a conjecture: substances strongly confined in CNTs might be retained at a solid-liquid critical point, which allows liquid directly and continuously transform into solid.^[31] This unique phase transition behavior, which deviates significantly from classical thermodynamics, also promotes the investigation of ice nanotubes (encapsulated water frozen into crystalline solid with tube-like structure) in theoretical research and potential applications in the past twenty years.^[32]

MD simulation was used to understand the theoretical mechanism of ice nanotubes. Takaiwa *et al.*^[33] reported that the driving force of water to fill CNTs with different diameters is also different. With the increase of the diameter of CNTs, water changes from vapor-like phase (in 0.8–1.0 nm diameter CNTs) to ice-like phase (in 1.1–1.2 nm diameter CNTs) and finally to bulk liquid phase (in CNTs with diameter larger than 1.4 nm). In 2016, Agrawal *et al.*^[34] explored the phase boundaries of ice nanotubes in SWNTs of different diameters by Raman spectroscopy. They used deposition method to construct the CNTs platform and probed the characters of single CNT by microRaman spectroscopy (Figure 4a). When water was added to the reservoirs, the open ends contacted with bulk water and the inner tube was gradually filled. A blue shift in the frequency of the Raman radial breathing mode (RBM) was observed, which can be assigned to the dynamic filling of water (Figure 4b). They also collected a complete data set (RBM frequency vs. temperature) to analysis the phase transition temperature for different diameter CNTs. The second RBM upshift (black line, Figure 4c) in the contour plot was indicated as the freezing transition of water from a liquid to a solid phase. Thus, they found that water in 1.05 nm-diameter SWNT actually freezes at 105–151 °C, which is much larger than theoretically predicted value. All these results indicate new opportunities for phase

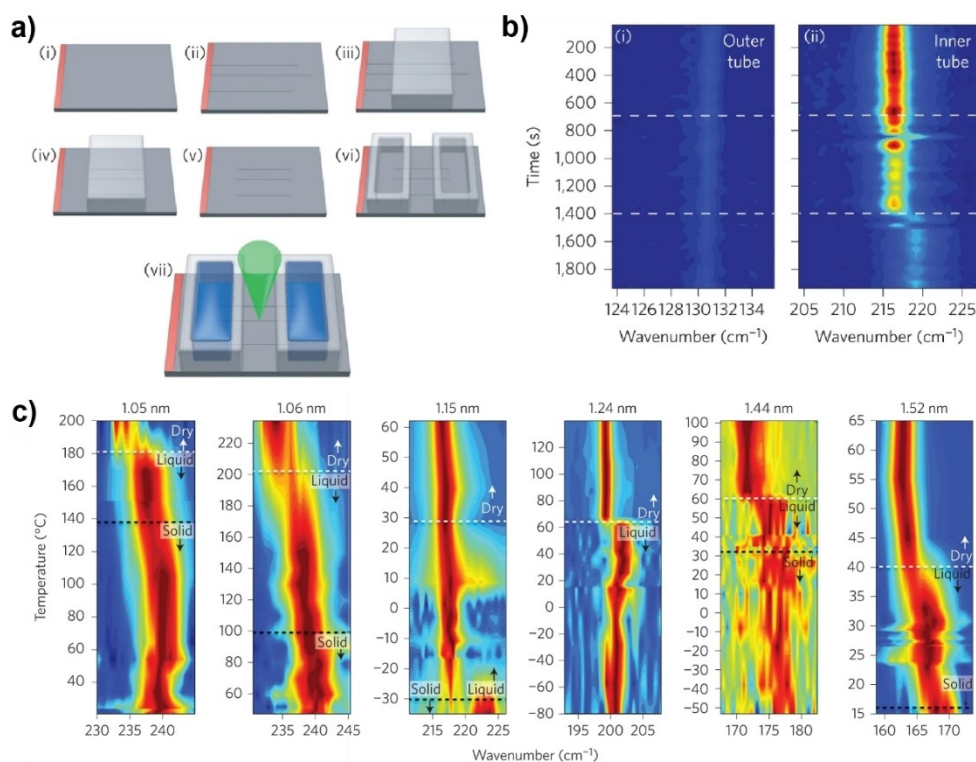


Figure 4. Phase transition of water in CNTs. a) Fabrication of the CNTs platform. b) Temporal study of the Raman radial breathing mode frequency showing the evolution of RBM frequency and intensities for the 1.15 nm-diameter CNT. c) Representative RBM frequency versus temperature for six tubes with different diameters showing the water-filled state transition. Reproduced with permission from Ref. [30], Copyright 2016, Springer Nature.

transitions of encapsulated fluid in CNTs. However, new theories and comprehensive supporting experimental data are still needed.

4. Applications of CNTs-Based Nanofluidic Devices

As mentioned above, the properties of the flow enhancement and the ion exclusion endow CNT-based devices with the most possibility to solve the water and energy problem. Although the performance of CNT membranes is comparable to commercial desalination membranes, how to scale up the membrane areas and maintain the mechanical stability is still an obstacle to apply to desalinate and produce electricity.^[4] In contrast, other innovative and interesting applications of CNTs nanofluidic device have been implemented during the last ten years.

4.1. Sensors

Field effect transistors (FETs) which amplify small changes such as the variation of surface potential due to the ligand binding by high intrinsic transistor gain, have been developed as a mature sensing platform. Nevertheless, the unavoidable fouling problem challenges FETs sensors when working in complex biological fluids. Using lipid bilayer embedded with CNTs as the

pH FETs coating, Chen *et al.*^[35] balanced the antifouling property and the sensing performance at the same time. The lipid membrane coated on the silicon nanoribbon was used to separate the fluids from the surface. The embedded 0.8 nm-diameter CNTs in the membrane served as channels for high proton permeability (Figure 5a, b). This approach provides the FETs sensor with long-term antifouling ability even in rather complex biological environment. Also, it illustrates that the tunable permeability of CNTs could be applied in the fabrication of sensing platforms.

The CNT-based devices are also used as DNA sensing platforms due to its robustness and tunability. Wu *et al.* reported a device embedded with ultrashort CNT by injection (Figure 1b) as a novel DNA sensor.^[17] The ssDNA was driven through the CNTs under an applied voltage. A remarkably large current blockades compared with that in α -hemolysin could be observed. They further validated the applicability of the device in detecting 5-hydroxymethylcytosine (5hmC) in ssDNA with the measurement of ionic current (Figure 5c). A significant current spike appeared in the blockade which represented the translocation of the modified part (Figure 5d). This strategy offers a powerful tool for 5hmC site detection which has an important role in tissue-specific gene expression. In 2014, Geng *et al.*^[18] also achieved DNA analysis by CNT-based devices. A similar set-up for single-channel conductance measurements (Figure 1d) was constructed by recording the spontaneous incorporation of the lipid-coated ultrashort CNTs. A current blockade would be recorded immediately when the ssDNA

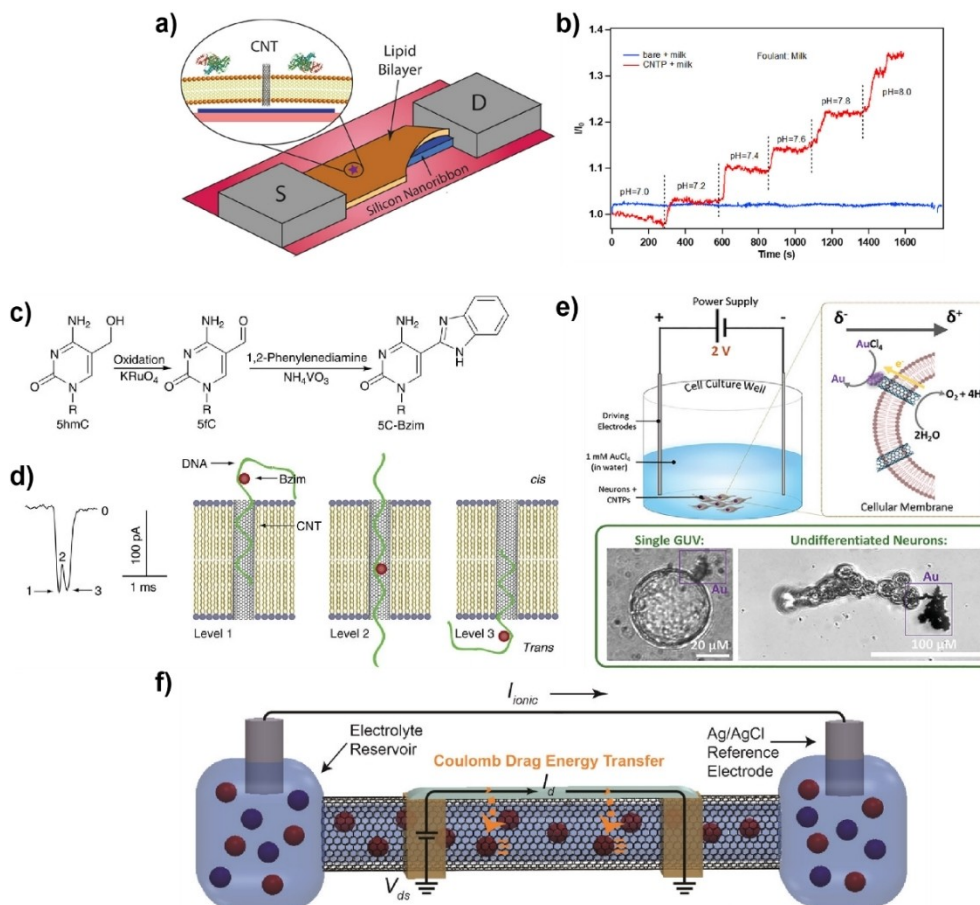


Figure 5. Applications of CNT-based nanofluidic devices. a) A silicon nanoribbon transistor-based pH sensor with a coating of antifouling lipid bilayer embedded with CNTs. Reproduced with permission from Ref. [31], Copyright 2019, American Chemical Society. b) pH responses of the silicon nanoribbons device with CNTs (red) after exposure to dilute milk for 60 h. Reproduced with permission from Ref. [31], Copyright 2019, American Chemical Society. c) 5hmC modification. Reproduced with permission from Ref. [17], Copyright 2013, Springer Nature. d) A characteristic type of current signature and diagram showing the translocation of benzoimidazole (Bzim)-modified 5hmC-containing DNA. Reproduced with permission from Ref. [17], Copyright 2013, Springer Nature. e) The experimental setup of CNTs as artificial TPMETs. Brightfield images show the Au deposition on single GUV and neurons. Reproduced with permission from Ref. [32], Copyright 2021, John Wiley and Sons. f) An individual SWNT connects two electrically isolated circuits. Coulomb drag energy transfers to the ions in the SWNT core (orange arrows). Reproduced with permission from Ref. [38], Copyright 2019, American Chemical Society.

passes through the nanochannel. It was also found that the DNA translocation speed is comparable to the biological nanopores, which also validated the possibility of this CNT-based device in DNA analysis.

4.2. Cell fate modulation

In addition to nanopore sensing, CNTs can also be used as a microelectrode immersed on cell membrane for redox modulation. Hicks *et al.*^[36] took advantage of CNTs as wireless bipolar electrodes (BPEs) due to their electrical conductivity and constructed artificial trans-plasma membrane electron transport systems (TPMETs) by embedding ultrashort CNTs in cell membrane (Figure 5e). Under the polarization of external potential, redox reactions occur at both ends of the BPE.^[37] The mechanism is similar to that of TPMETs which can be described as the reduction of the oxidants extracellularly while the oxidation of reductants intracellularly. They inserted the

ultrashort lipid-coating CNTs into the membranes of giant unilamellar vesicles (GUVs) as a simplified cellular model and immersed them in 1 mM gold chloride solution with two driving electrodes. After the application of external voltage for 1 h, the gold deposition at the GUV embedded with CNTs could be observed which illustrates the function of CNTs as nano-scale BPEs. Finally, they used cell-friendly voltage to treat the live cells embedded with CNTs in 1 mM gold chloride. The deposition of gold at the membrane surface can also be observed. This interesting research not only offers a new method to modulate cell redox behavior by CNTs device, but also expands the application of CNTs devices as artificial TPMETs in electrochemical therapeutics.

4.3. Biomimetic ion channel

Shepard *et al.* constructed a SWNT-based FET to mimic ion pump.^[38] They used two gold electrodes under the SWNT to

apply drain-source potential (V_{ds}) and set two electrolyte reservoirs connecting the ends of the SWNT with reference electrodes to measure ionic currents (Figure 5f). When applying V_{ds} , electronic current will flow along the SWNT shell. The ions in electrolyte are pumped into the SWNT by the solid-state electronic input, just like an electrically actuated biomimetic ion pump. It is Coulomb drag energy transferring to the ions in the SWNT core that causing the ionic current without requiring electrolyte potential or pressure gradients. This device also affords new chance in biosensing and filtration application with controllability and selectivity.

As the CNTs can realize water fast flow with ion exclusion, CNT-based devices have the potential to mimic the Aquaporin-1. A response of biological mechanosensitive ion channels is also observed in CNT-based devices with pressure sensitivity.^[39] Using a nanomanipulator, a single CNT was inserted into a hole drilled in a silicon membrane and sealed robustly between two reservoirs. Pressure drop was applied by a pressure controller connected to the reservoir and caused pressure-driven ionic current. Quadratically pressure-modulation of the conductance of CNTs is found in this artificial system, which is similar with the response of mechanosensitive biological channels. The nanometric spatial resolution to pressure signals of this system also provide a way to develop sensing devices for touch.

5. Summary and Perspective

Nanofluidics has come to its age with the development of nanofabrication technology and advanced instruments for the investigation of mass transport. Among numerous materials, CNTs provide an ideal channel platform to study unique nanofluidic behaviors. Since the early 2000s, studies on the properties of nanofluids in CNTs have showed many interesting results, such as flow enhancement of water, large proton fluxes, icelike water phases and high ion exclusion.

These exciting discoveries provide various potential applications of CNT-based nanofluidic devices: 1) seawater desalination due to their strongly rejection of chloride ion;^[5,40] 2) sensors;^[7a,35,41] 3) proton conductor materials in energy transduction due to their ultrafast proton transport characteristic;^[19] 4) molecular nanovalves due to their novel gas adsorption properties;^[32d] 5) artificial channel proteins with stable insertion and tunability.^[18,38–39,42] 6) DNA sequencing and DNA-damage sensing due to their high signal-to-noise ratio;^[17] 7) cell fate modulation. CNT BPEs make it possible to artificially transport trans-membrane electron, which offers the opportunity to reprogram cellular metabolism.^[36] 8) Use for molecular sieving owing to their structural rigidity and the flexibility of the absorbate.^[43]

Nevertheless, grand challenges still exist and hinder the development of CNT-based nanofluidic devices. First of all, the reproducibility in device fabrication needs to be improved. The difference in the inner diameter of CNTs and ubiquitous surface defects may lead to data bias. Besides, knowledge gaps have recently emerged in understanding these bizarre observations of nanofluidic. As an immature field, the investigation of CNT-

based nanofluidic devices still have a long way to go and demands the development of advanced synthesis methods and characterization techniques for next steps.

Acknowledgments

This work was supported by financial support from the Natural Science Foundation of Beijing (no. JQ19009), the National Natural Science Foundation of China (Grant Nos. 22125406, 22074149, 21790053), and the Strategic Priority Research Program of Chinese Academy of Sciences (XDB30000000).

Conflict of Interest

The authors declare no conflict of interest.

Data Availability Statement

Research data are not shared.

Keywords: carbon nanotubes · ion transport · nanofluid · nanofluidic devices · water transport

- [1] J. K. Holt, H. G. Park, Y. M. Wang, M. Stadermann, A. B. Artyukhin, C. P. Grigoropoulos, A. Noy, O. Bakajin, *Science* **2006**, *312*, 1034–1037.
- [2] L. Fumagalli, A. Esfandiari, R. Fabregas, S. Hu, P. Ares, A. Janardan, Q. Yang, B. Radha, T. Taniguchi, K. Watanabe, G. Gomila, K. S. Novoselov, A. K. Geim, *Science* **2018**, *360*, 1339–1342.
- [3] J. D. Feng, K. Liu, M. Graf, D. Dumcenco, A. Kis, M. Di Ventra, A. Radenovic, *Nat. Mater.* **2016**, *15*, 850–855.
- [4] L. Bocquet, *Nat. Mater.* **2020**, *19*, 254–256.
- [5] Y. H. Li, Z. W. Li, F. Aydin, J. N. Quan, X. Chen, Y. C. Yao, C. Zhan, Y. F. Chen, T. A. Pham, A. Noy, *Sci. Adv.* **2020**, *6*, eaba9966.
- [6] a) X. Tong, S. Liu, J. Crittenden, Y. S. Chen, *ACS Nano* **2021**, *15*, 5838–5860; b) Z. Zhang, L. Wen, L. Jiang, *Nat. Rev. Mater.* **2021**, *6*, 622–639.
- [7] a) C. Lu, C. Hu, C. L. Ritt, X. Hua, J. Sun, H. Xia, Y. Liu, D.-W. Li, B. Ma, M. Elimelech, J. Qu, *J. Am. Chem. Soc.* **2021**, *143*, 14242–14252; b) R. Peng, Y. Pan, B. Liu, Z. Li, P. Pan, S. Zhang, Z. Qin, A. R. Wheeler, X. Tang, X. Liu, *Small* **2021**, *17*, 2100383.
- [8] S. Marion, A. Radenovic, *Nat. Mater.* **2020**, *19*, 1043–1044.
- [9] a) A. Keerthi, A. K. Geim, A. Janardan, A. P. Rooney, A. Esfandiari, S. Hu, S. A. Dar, I. V. Grigorieva, S. J. Haigh, F. C. Wang, B. Radha, *Nature* **2018**, *558*, 420–424; b) R. Kidambi Piran, P. Chaturvedi, K. Moehring Nicole, *Science* **2021**, *374*, eabd7687; c) Y. Xue, Y. Xia, S. Yang, Y. Alsaied, Y. Fong King, Y. Wang, X. Zhang, *Science* **2021**, *372*, 501–503; d) T. Emmerich, K. S. Vasu, A. Niguès, A. Keerthi, B. Radha, A. Siria, L. Bocquet, *Nat. Mater.* **2022**, *21*, 696–702; e) L. Saini, S. S. Nemala, A. Rathi, S. Kaushik, G. Kalon, *Nat. Commun.* **2022**, *13*, 498.
- [10] K. Celebi, J. Buchheim, R. M. Wyss, A. Droudian, P. Gasser, I. Shorubalko, J. I. Kye, C. Lee, H. G. Park, *Science* **2014**, *344*, 289–292.
- [11] A. K. Geim, I. V. Grigorieva, *Nature* **2013**, *499*, 419–425.
- [12] A. Esfandiari, B. Radha, F. C. Wang, Q. Yang, S. Hu, S. Garaj, R. R. Nair, A. K. Geim, K. Gopinadhan, *Science* **2017**, *358*, 511–513.
- [13] a) F. Calabro, *MRS Bull.* **2017**, *42*, 289–293; b) B. Corry, *MRS Bull.* **2017**, *42*, 306–310; c) S. K. Kannam, P. J. Davis, B. D. Todd, *MRS Bull.* **2017**, *42*, 283–288; d) M. Majumder, A. Siria, L. Bocquet, *MRS Bull.* **2017**, *42*, 278–282; e) H. Min, Y. T. Kim, C. Y. Lee, *MRS Bull.* **2017**, *42*, 300–305; f) S. Faucher, N. Aluru, M. Z. Bazant, D. Blankschtein, A. H. Brozena, J. Cumings, J. P. de Souza, M. Elimelech, R. Epsztein, J. T. Fourkas, A. G. Rajan, H. J. Kulik, A. Levy, A. Majumdar, C. Martin, M. McEldrew, R. P. Misra, A. Noy, T. A. Pham, M. Reed, E. Schwegler, Z. Siwy, Y. H. Wang, M. Strano, *J. Phys. Chem. C* **2019**, *123*, 21309–21326.

- [14] C. Y. Lee, W. Choi, J. H. Han, M. S. Strano, *Science* **2010**, *329*, 1320–1324.
- [15] H. T. Liu, J. He, J. Y. Tang, H. Liu, P. Pang, D. Cao, P. Krstic, S. Joseph, S. Lindsay, C. Nuckolls, *Science* **2010**, *327*, 64–67.
- [16] L. Sun, R. M. Crooks, *J. Am. Chem. Soc.* **2000**, *122*, 12340–12345.
- [17] L. Liu, C. Yang, K. Zhao, J. Y. Li, H. C. Wu, *Nat. Commun.* **2013**, *4*, 2989.
- [18] J. Geng, K. Kim, J. F. Zhang, A. Escalada, R. Tunuguntla, L. R. Comolli, F. I. Allen, A. V. Shnyrova, K. R. Cho, D. Munoz, Y. M. Wang, C. P. Grigoropoulos, C. M. Ajo-Franklin, V. A. Frolov, A. Noy, *Nature* **2014**, *514*, 612–615.
- [19] R. H. Tunuguntla, F. I. Allen, K. Kim, A. Belliveau, A. Noy, *Nat. Nanotechnol.* **2016**, *11*, 639–644.
- [20] K. Falk, F. Sedlmeier, L. Joly, R. R. Netz, L. Bocquet, *Nano Lett.* **2010**, *10*, 4067–4073.
- [21] G. Hummer, J. C. Rasaiah, J. P. Noworyta, *Nature* **2001**, *414*, 188–190.
- [22] M. Majumder, N. Chopra, R. Andrews, B. J. Hinds, *Nature* **2005**, *438*, 44–44.
- [23] E. Secchi, S. Marbach, A. Nigues, D. Stein, A. Siria, L. Bocquet, *Nature* **2016**, *537*, 210–213.
- [24] R. H. Tunuguntla, R. Y. Henley, Y. C. Yao, T. A. Pham, M. Wanunu, A. Noy, *Science* **2017**, *357*, 792–796.
- [25] C. A. Wraight, *Biochim. Biophys. Acta Bioenerg.* **2006**, *1757*, 886–912.
- [26] F. Fornasiero, H. G. Park, J. K. Holt, M. Stadermann, C. P. Grigoropoulos, A. Noy, O. Bakajin, *Proc. Natl. Acad. Sci. USA* **2008**, *105*, 17250–17255.
- [27] S. F. Buchsbaum, M. L. Jue, A. M. Sawvel, C. T. Chen, E. R. Meshot, S. J. Park, M. Wood, K. J. Wu, C. L. Bilodeau, F. Aydin, T. A. Pham, E. Y. Lau, F. Fornasiero, *Adv. Sci.* **2021**, *8*, 2001802.
- [28] Z. W. Li, Y. H. Li, Y. C. Yao, F. Aydin, C. Zhan, Y. F. Chen, M. Elimelech, T. A. Pham, A. Noy, *ACS Nano* **2020**, *14*, 6269–6275.
- [29] E. Secchi, A. Nigues, L. Jubin, A. Siria, L. Bocquet, *Phys. Rev. Lett.* **2016**, *116*, 154501.
- [30] Y. C. Yao, A. Taqieddin, M. A. Alibakhshi, M. Wanunu, N. R. Aluru, A. Noy, *ACS Nano* **2019**, *13*, 12851–12859.
- [31] P. Ball, *Nature* **1993**, *361*, 297.
- [32] a) K. Koga, G. T. Gao, H. Tanaka, X. C. Zeng, *Nature* **2001**, *412*, 802–805; b) Y. Maniwa, H. Kataura, M. Abe, S. Suzuki, Y. Achiba, H. Kira, K. Matsuda, *J. Phys. Soc. Jpn.* **2002**, *71*, 2863–2866; c) J. E. Bai, J. Wang, X. C. Zeng, *Proc. Natl. Acad. Sci. USA* **2006**, *103*, 19664–19667; d) Y. Maniwa, K. Matsuda, H. Kyakuno, S. Ogasawara, T. Hibi, H. Kadowaki, S. Suzuki, Y. Achiba, H. Kataura, *Nat. Mater.* **2007**, *6*, 135–141; e) J. Shiomi, T. Kimura, S. Maruyama, *J. Phys. Chem. C* **2007**, *111*, 12188–12193; f) M. Kuehne, S. Faucher, M. Liew, Z. Yuan, S. X. Li, T. Ichihara, Y. Zeng, P. Gordichuk, V. B. Koman, D. Kozawa, A. Majumdar, M. S. Strano, *J. Phys. Chem. C* **2021**, *125*, 25717–25728.
- [33] D. Takaiwa, I. Hatano, K. Koga, H. Tanaka, *Proc. Natl. Acad. Sci. USA* **2008**, *105*, 39–43.
- [34] K. V. Agrawal, S. Shimizu, L. W. Drahushuk, D. Kilcoyne, M. S. Strano, *Nat. Nanotechnol.* **2017**, *12*, 267–273.
- [35] X. Chen, H. N. Zhang, R. H. Tunuguntla, A. Noy, *Nano Lett.* **2019**, *19*, 629–634.
- [36] J. M. Hicks, Y. C. Yao, S. Barber, N. Neate, J. A. Watts, A. Noy, F. J. Rawson, *Small* **2021**, *17*, 2102517.
- [37] P. Yu, H. Wei, P. Zhong, Y. Xue, F. Wu, Y. Liu, J. Fei, L. Mao, *Angew. Chem. Int. Ed.* **2020**, *59*, 22652–22658; *Angew. Chem.* **2020**, *132*, 22841–22847.
- [38] J. Rabinowitz, C. Cohen, K. L. Shepard, *Nano Lett.* **2020**, *20*, 1148–1153.
- [39] A. Marcotte, T. Mouterde, A. Nigues, A. Siria, L. Bocquet, *Nat. Mater.* **2020**, *19*, 1057–1061.
- [40] Y. Q. Hou, M. Wang, X. Y. Chen, X. Hou, *Nano Res.* **2021**, *14*, 2171–2178.
- [41] a) S. Ghosh, A. K. Sood, N. Kumar, *Science* **2003**, *299*, 1042–1044; b) Y. Wang, Z. Wang, L. Wang, T. Tong, X. Zhang, S. Fang, W. Xie, L. Liang, B. Yin, J. Yuan, J. Zhang, D. Wang, *Nano Lett.* **2022**, *22*, 2147–2154.
- [42] a) G. Liu, B. Zhou, J. Liu, H. Zhao, *Sustainability* **2021**, *13*, 102; b) Y.-C. Yao, Z. Li, A. J. Gillen, S. Yosinski, M. A. Reed, A. Noy, *J. Chem. Phys.* **2021**, *154*, 204704.
- [43] H. Qu, A. Rayabharam, X. J. Wu, P. Wang, Y. F. Li, J. Fagan, N. R. Aluru, Y. H. Wang, *Nat. Commun.* **2021**, *12*, 310.

Manuscript received: June 1, 2022

Revised manuscript received: October 5, 2022